Superparamagnetism in carbon-coated Co particles produced by the Kratschmer carbon arc process

M. E. McHenry*
Department of Materials Science and Engineering, Carnegie Mellon University, Pittsburgh, Pennsylvania 15213-3890

S. A. Majetich
Department of Physics, Carnegie Mellon University, Pittsburgh, Pennsylvania 15213-3890

J. O. Artman
Department of Physics, Carnegie Mellon University, Pittsburgh, Pennsylvania 15213-3890
and Department of Electrical and Computer Engineering, Carnegie Mellon University, Pittsburgh, Pennsylvania 15213-3890

M. DeGraef
Department of Materials Science and Engineering, Carnegie Mellon University, Pittsburgh, Pennsylvania 15213-3890

S. W. Staley
Department of Chemistry, Carnegie Mellon University, Pittsburgh, Pennsylvania 15213-3890
(Received 12 October 1993)

A process based on the Kratschmer-Huffman carbon arc method of preparing fullerenes has been used to generate carbon-coated cobalt and cobalt carbide nanocrystallites. Magnetic nanocrystallites are extracted from the soot with a gradient field technique. For Co/C composites, structural characterization by x-ray diffraction and high-resolution transmission electron microscopy reveals the presence of a fcc Co phase, graphite, and a minority Co_2C phase. The majority of Co nanocrystals exists as nominally spherical particles, 0.5–5 nm in radius. Hysteretic and temperature-dependent magnetic response, in randomly and magnetically aligned powder samples frozen in epoxy reveals fine-particle magnetism associated with monodomain Co particles. The magnetization exhibits a unique functional dependence on H/T, and hysteresis below a blocking temperature, $T_B \cong 160$ K. Below T_B, the temperature dependence of the coercivity is given by $H_c = H_{ci}[1-(T/T_B)^{1/2}]$, with $H_{ci} \cong 450$ Oe.

INTRODUCTION

The breakneck pace at which the field of fullerene[1] synthesis and chemistry has been proceeding is in large part due to the discovery of the Kratschmer carbon arc process,[2] whereby macroscopic amounts of the C_{60}, C_{70}, and higher fullerene cage molecules can be produced. This discovery was followed by the discovery of tubular fullerenes[3] and multiple-shell fullerenes[4] as byproducts of the carbon arc process. Yet another important development has been the discovery of techniques for the endohedral doping of fullerenes[5] produced by the carbon arc. An exciting adjunct of endohedral fullerene production is the formation of carbon-coated metal or metal carbide nanocrystallites. The first of this new class of compounds to be reported was the LaC_2 nanoparticle.[6-7] An adherent multiple-shell graphitic carbon coating on these particles has led to them being classified as "giant fullerenes." Our group has recently described the preparation of rare-earth carbide nanocrystallites,[8] as well as a method for their separation which takes advantage of the large paramagnetic moments of the rare-earth species. Here we report on the synthesis and separation of similar carbon-coated *ferromagnetic* transition metal and transition-metal carbide nanocrystallites. Such carbon-coated magnetic-metal nanocrystallites are of interest for potential applications in which ferromagnetic iron-oxide particles are currently used: i.e., in magnetic data storage, for magnetic toner in xerography, in ferrofluids, and as contrast agents in magnetic resonance imaging. The magnetic particles produced by the carbon arc process are predominantly monodomain. The carbon coating provides an effective oxidation barrier. Here we describe also measurements on the structure and magnetic properties of these carbon coated fcc Co nanocrystals as well as interesting manifestations of fine-particle magnetism, including superparamagnetic response. Our data provide the first link between fullerene-related nanocrystals and the studies of fine-particle magnetism with the aim of producing materials interesting for magnetic recording.

EXPERIMENTAL PROCEDURE

In the carbon arc process $\frac{1}{4}$ in. diameter graphite rods were first drilled and packed with a mixture of metal oxide powder (in this case Co_3O_4) and a combination of graphite powder and graphite cement. We used a 1:1 volume ratio of Co_3O_4 and graphite powder bound together with a minimal amount of graphite cement. The rods were then baked overnight at 300 °C to drive off water vapor and to cure the graphite cement. We estimated our starting materials had an ~0.04 Co/C molar ratio, consistent with the La/C molar ratio of Ref. 2. The rods

were then placed in the upper electrode position in dc carbon arc,[5] and a carbon counterelectrode was employed. The rods were consumed under arc conditions of 100 A and 30 V, along with a helium gas pressure of 125 Torr. In general, in the presence of excess carbon, a metal oxide, M_xO_y, is reduced in the plasma provided by the arc in accordance with the reaction

$$M_xO_y + yC \rightleftharpoons xM + yCO \ , \tag{1}$$

which is favored in the high temperature of the plasma. The deposited soot is a mixture of graphitic particles, carbon-coated nanocrystallites, and various fullerenes. It is of course also possible to synthesize a metal carbide phase as observed for Gd- and Ho-containing materials.[8] Whether or not a carbide is formed depends on the metal/carbon phase diagram, and cobalt is a poor carbide former.

The raw soot was first ground to a fine, micrometer-sized powder with a mortar and pestle. The powder was then passed through a magnetic-field gradient to separate magnetic from nonmagnetic species. We recall that a ferromagnetic particle with magnetization **M** experiences a magnetic force:

$$\mathbf{F}_M = (\mathbf{M}\cdot\nabla)\mathbf{H} \ . \tag{2}$$

The separator consisted of a funnel, an electrically grounded aluminum tube with a pair of $1\times1\times\frac{1}{2}$ in.^{3} neodymium iron boron permanent magnets ($M_r = 1.3$ T, Crucible Materials Corporation) on either side, and a pair of collection flasks. The grounded metal tube was necessary to prevent electrostatic charging of the powder.

The tube was positioned between the magnets to maximize $\mathbf{F}_M$. When small amounts of powder were poured through the apparatus the magnetic species were suspended, while the nonmagnetic fraction passed through. The collection bottles were switched, and the tube was moved away from the magnets to release the magnetic powder. Unlike the case for rare-earth carbides, where a significant non-magnetic fraction was separated, ~95% by volume of the Co-containing soot was magnetic after the first pass. However, as will be discussed later, only a small fraction of this magnetically responding powder is ferromagnetic Co. Thus it appears that the "magnetic" species filtered contains ferromagnetic Co particles embedded in carbon. Furthermore, the magnetic "filtrate" contains a mixture of the magnetic nanocrystallites discussed here, along with small amounts of endohedral fullerenes. Most of these latter compounds were removed by extraction in carbon disulfide.[9]

X-ray diffraction (XRD) of the nanocrystallites with a Rigaku diffractometer revealed peaks [Fig. 1(a)] suggestive of the presence of the fcc cobalt phase, along with the predominant graphitic peaks and a broadened peak at small angles (not shown) characteristic of the fullerenes. No evidence was found by XRD for the hcp Co phase, or for metastable cobalt carbides; however, some TEM evidence for a minority Co_2C phase is noted. We note that the fcc as opposed to an hcp cobalt phase is observed in thin-film microstructures.

The structure and morphology of the magnetic powder

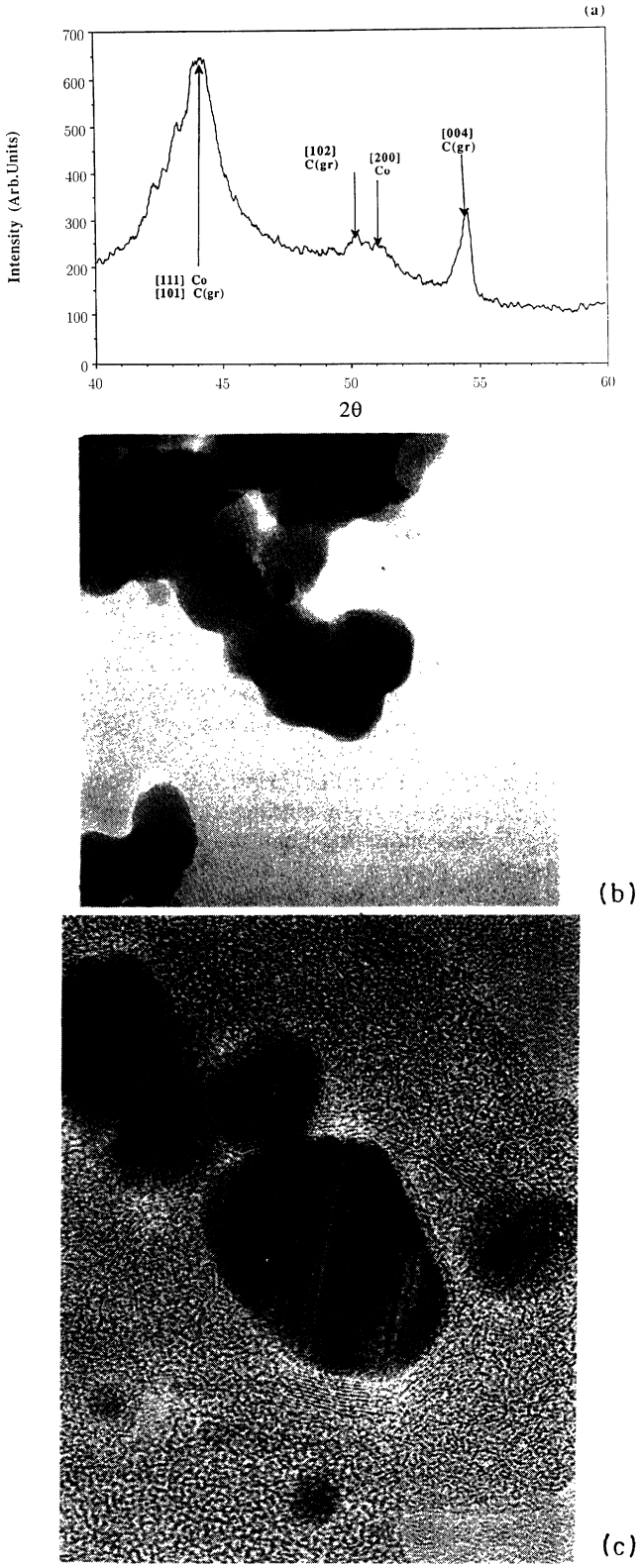

FIG. 1. (a) X-ray diffraction pattern of the magnetically separated powder taken with a Rigaku diffractometer using copper K_α and K_β radiation fcc Co and hexagonal graphite peaks are identified. (b) Transmission electron micrograph of a cobalt nanocrystallite enclosed by several graphitic sheets, taken with a JEOL 400 high-resolution TEM. (c) HRTEM micrograph of an individual Co nanocrystallite showing stacking faults.

were examined by electron microscopy. Energy dispersive x-ray fluorescence spectroscopy indicated that the cobalt was uniformly distributed in the sample. Scanning electron microscopy revealed submicron-sized nominally spherical particles. Closer inspection [Fig. 1(b) and 1(c)] was made with a JEOL 4000, 400 keV, high-resolution transmission electron microscope (HRTEM). Samples were prepared by dispersing the powder in methanol with the aid of ultrasound and then drying a drop of the solution on an amorphous carbon-coated copper grid. The 0.5–5-nm radius observed is somewhat smaller than previously observed for Gd_2C_3 nanocrystallites which were observed to be some 5–25 nm in radius. We observed, enclosed in amorphous carbon, cobalt nanocrystallites encapsulated in 5–10 curved graphitic shells [Fig. 1(b)], along with a small fraction of similarly coated Co_2C crystallites. Fullerene-sized carbon clusters were also seen. Curved, layered graphite structures appeared throughout the sample, but nodules rather than tubes predominated. Unlike the observations for similarly produced LaC_2 nanocrystallites,[1,2] no voids were observed between the metal and carbon phases. Many Co particles were observed to be faulted. Our particle sizes are roughly equivalent to those observed by Bethune *et al.*[10] but we did not observe the weblike morphology of carbon nanotubes that they have reported.

Magnetization data for the enriched Co nanocrystallite powder samples have been obtained employing a quantum design superconducting-quantum-interference-device magnetometer. Powders containing the nanocrystallites were immobilized by epoxy. Samples containing randomly aligned particles as well as those allowed to align in the field provided by a pair of FeNdB permanent magnets were prepared for observation. $M(H,T)$ has been determined in solenoidal fields between ± 5 T and for temperatures ranging from 4–300 K.

RESULTS AND DISCUSSION

Figure 2(a) shows magnetization vs field data for Co nanocrystallites randomly oriented in epoxy at temperatures of 5, 10, 15, 20, 25, 50, 100, and 200 K. Notice the nonsaturated magnetic behavior which progressively increases at lower temperatures. Figure 2(b) shows the same $M(H)$ curves plotted against H/T on the horizontal axis resulting in a universal curve. This scaling is consistent with superparamagnetic response, though it is strictly only a true scaling at low fields for temperatures above the blocking temperature T_B. Later we will show that T_B is ~ 160 K. The saturation moment of 0.17 emu (for an ~ 18 mg sample) corresponds to an apparent saturation magnetization of ~ 10 emu/g. From a comparison with the 0-K saturation magnetization, $\sigma_0 = 162.5$ emu/g (1.435×10^3 emu/cm^3) for pure fcc Co (Ref. 11) we estimate that our sample contains $\sim 6\%$ by weight of ferromagnetic Co. The universal curve of Fig. 2(b) can be fit to a Langevin function L using the relation

$$\frac{M}{M_0} = L(a) = \coth(a) - \frac{1}{a} , \tag{3}$$

where $M_0 = 10$ emu/g and $a = \mu H/kT$. The effective moment μ is given by the product $M_s\langle V\rangle$ where M_s is the saturation magnetization and $\langle V\rangle$ is the average particle volume. Using data only for temperatures above 160 K, for which the sample is truly in the superparamagnetic regime, a least-squares fit to the magnetization data reveals a moment $\mu \cong 1\times 10^{-16}$ emu or $\cong 1.1\times 10^4\ \mu_B$, which is consistent with ~ 6000 Co atoms per particle. Again using the 0-K value of the saturation magnetization, $\sigma_0 = 1435$ emu/cm^3, we estimate an average particle volume $\langle V\rangle \cong 7\times 10^{-20}$ cm^3 corresponding to spherical particles with radius $r \cong 2.5$ nm, in excellent agreement with the TEM observations.

Figure 3(a) shows magnetic hysteresis for the same randomly aligned nanocrystalline Co sample viewed on a smaller field scale. The sheared and significantly rounded nature of the $M(H)$ loops at 5 K can be associated with both the demagnetization factors for nominally spherical particles (shearing) and significant rotational barriers to saturation (rounding). Notice that at the higher temperature of 50 K, the hysteresis is significantly reduced and the rounding is less significant, but the shearing is the same. These observations are consistent with thermally activated rotational processes. Figure 3(b) shows the hys-

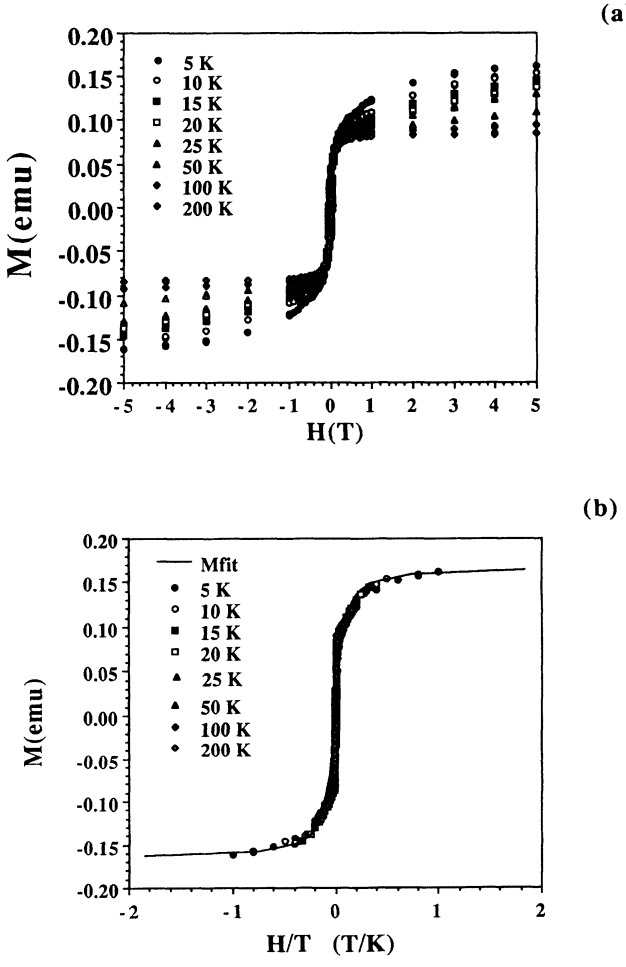

FIG. 2. (a) Magnetization vs applied field at temperatures of 5, 10, 15, 20, 25, 50, 100, and 200 K for nanocrystalline Co/C particles randomly oriented and immobilized by epoxy. (b) These magnetization data plotted as a function of H/T.

teretic response for Co nanocrystallites magnetically aligned with easy axis parallel to the field. Again some demagnetization-related shearing is observed in these loops. $M(H)$ for the aligned material, however, exhibits significantly reduced rounding, consistent with the reduction of the rotational barriers to saturation. The loops, therefore, reflect a simple 180° switching of the magnetization vector in the monodomains (i.e., nearly square loops). Note that the coercivity H_c is the same for the aligned and unaligned samples at similar temperatures.

Figure 4 shows the variation of the coercivity with temperature for both the aligned and unaligned samples. It is apparent from this figure that the coercivity is strongly temperature dependence but independent of the magnetic alignment. The inset to Fig. 4 shows that at low temperatures the coercivity obeys the relation

$$H_c = H_{ci}\left[1-\left[\frac{T}{T_B}\right]^{1/2}\right], \tag{4}$$

with a zero temperature (intrinsic) coercivity $H_{ci}\cong 450$ Oe and a blocking temperature T_B of ~ 160 K. The deviation from this temperature dependence at higher temperatures is thought to be due to the spread of the particle sizes. The value of the coercivity H_c at 77 K is ~ 130 Oe, consistent with the observation for similarly sized Co particles.[12]

In the theory of superparamagnetism,[13,14] the blocking temperature represents the temperature at which the metastable hysteretic response is lost for a particular experimental time frame. In other words, below the blocking temperature hysteretic response is observed since thermal activation is not sufficient to allow the immediate alignment of particle moments with the applied field. For spherical particles the rotational energy barrier to alignment is given by the magnetic anisotropy energy per unit volume K multiplied by the particle volume V. For hysteresis loops taken over ~ 1 h, the blocking temperature should roughly satisfy the relationship

$$T_B = \frac{K\langle V\rangle}{30k_B}. \tag{5}$$

The factor of 30 represents $\ln(\omega_0/\omega)$, where ω is the inverse of the experimental time constant ($\sim 10^{-4}$ Hz) and ω_0 an attempt frequency (~ 1 GHz). Using the 0-K value of the magnetic anisotropy for fcc Co ($K=-2.7\times 10^6$ ergs/cm^3),[15,16] we calculate an average volume $\langle V\rangle \cong 2.5\times 10^{-19}$ cm^3, corresponding to mean particle radius $r\cong 3.9$ nm. This is again in excellent agreement

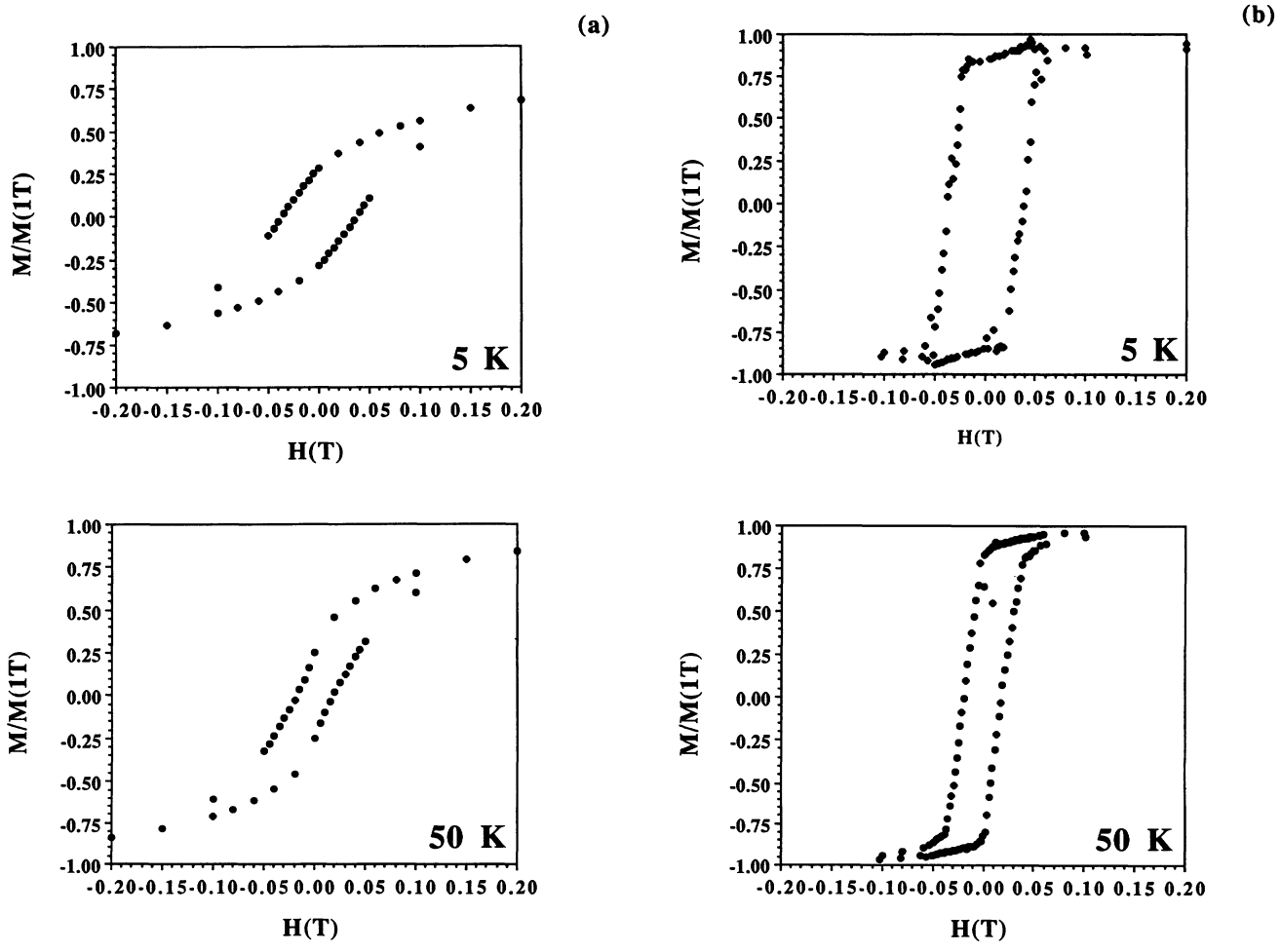

FIG. 3. Low-field magnetization curves at 5 and 50 K for Co/C particles (a) randomly oriented and (b) magnetically aligned.

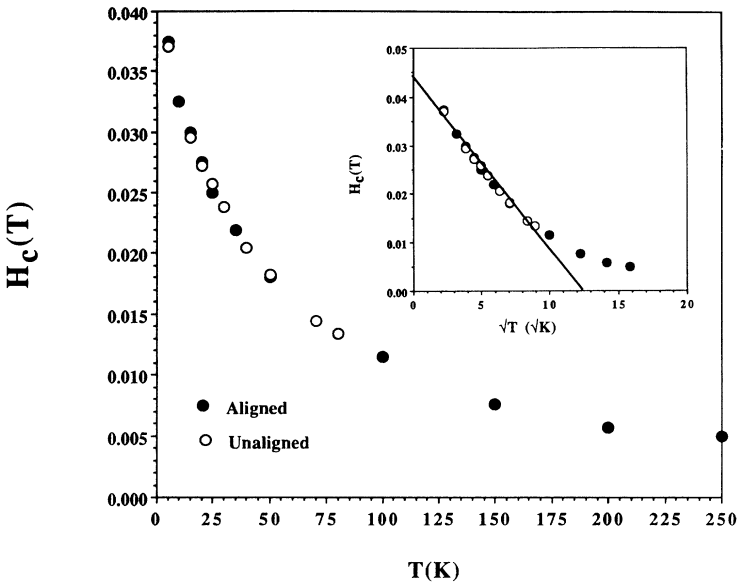

FIG. 4. Temperature dependence of the coercivity H_c for aligned and unaligned particles. The inset shows $H_c(T)$ to obey a $\sqrt{T}$ dependence with a blocking temperature T_B of ~ 160 K.

with both the TEM observations and the Langevin function fits. In future work we will also report on magnetic relaxation in the frozen state for $T < T_B$. This relaxation is observed to be logarithmic in time, consistent with a distributed set of activation energy barriers as might be expected for distributed particle sizes.

This work on Co nanoparticles in some respects parallels recent work on γ-Fe_2O_3 particles[17,18] for which similar superparamagnetic response can be observed[19] for similarly sized particles. It is interesting to note that fine-particle Co with CoO coatings are observed to exhibit exchange bias[20] due to interfacial interactions between ferromagnetic Co-metal antiferromagnetic CoO. In these systems, hysteresis loops are displaced along the field axis. The absence of such a displacement in our data can be taken as implying that our Co particles are completely reduced. Further, the substantial value (~ 450 Oe) of the 0-K coercivity in carbon-coated Co nanoparticles implies that current models explaining such large coercivities, including: (1) exchange coupling mediated through the matrix and (2) interfacial interactions, should be reconsidered in light of these results.

Our model considers only a uniaxial anisotropy K. We suspect that magnetocrystalline anisotropy is the primary determinant of the rotational energy barriers. However, further work is necessary to definitively assess the contribution due to magnetostatic energy in elongated or acicular particles and magnetostriction in stressed materials. TEM analysis has thus far indicted monodisperse and spherical particles for fcc Co[C] but with a significant fraction of stacking faults. The similarity between our coercivity values and those observed earlier[12] and attributed to magnetocrystalline anisotropy suggests that the same anisotropy mechanism may be also operative in our particles. The spherically shaped particles would seem to preclude a large contribution from shape anisotropy.

TABLE I. Particle size inferred from various magnetic measurements as compared with TEM analysis.

	Langevin fit	Blocking temperature	Coercivity (Ref. 12)	TEM analysis
Particle radius (nm)	2.5	3.9	1.5–2	0.5–5

CONCLUSIONS

The Kratschmer-Huffman carbon arc method of preparing fullerenes has been used to generate carbon-coated cobalt and cobalt carbide nanocrystallites, which are then collected using a magnetic separation technique. These particles contain fcc cobalt as the primary ferromagnetic species, with a nominally spherical particle morphology with a 0.5–5-nm radius from TEM. These small monodomain particles exhibit superparamagnetic response with magnetic hysteresis observed only at temperatures $T < T_B$ where $T_B \cong 160$ K. Analysis of the magnetic relaxation kinetics and from that the determination of the blocking temperature, as well as Langevin fits to the superparamagnetic response suggest the presence of superparamagnetic particles with a mean radius of 3.9 and 2.5 nm, respectively, as summarized in Table I. These particle radii are in excellent agreement with observations made by TEM, and with prior measurements of fine-particle magnetism in fcc Co particles.

ACKNOWLEDGMENTS

M.E.M. and S.A.M. would like to thank the National Science Foundation for support through NYI Awards Nos. DMR-9258450 and DMR-9258308, respectively. This material is also based (in part) upon work supported by the National Science Foundation under Grant No. ECD-8907068. The assistance of the Carnegie Mellon University SURG program, and the participation of the CMU members have been invaluable. In addition we would like to thank L. Berger, N. T. Nuhfer, R. Sutton, E. Brunsman, B. Diggs, S. Kirkpatrick, J. Williams, and B. Brunett, for technical assistance.

*Author to whom all correspondence should be addressed.

[1]H. W. Kroto, J. R. Heath, S. C. O'Brien, R. F. Curl and R. E. Smalley, Nature **318**, 162 (1985).

[2]W. Kratschmer, L. D. Lamb, K. Fostiropoulos, and D.R. Huffman, Nature **347**, 354 (1990).

[3]S. Ijima, Nature **354**, 57 (1991).

[4]D. Ugarte, Nature **359**, 707 (1992); H. W. Kroto, *ibid.* **359**, 6701 (1992).

[5]Y. Chai, T. Guo, C. Jin, R. E. Haufler, L. P. F. Chibante, J. Fure, L. Wang, J. M. Alford, and R. E. Smalley, J. Phys. Chem. **95**, 7564 (1991).

[6]Rodney S. Ruoff, Donald C. Lorents, Bryan Chan, Ripudaman Malhotra, and Shekhar Subramoney, Science **259**, 346 (1993).

[7]M. Tomita, Y. Saito, and T. Hayashi, Jpn. J. Appl. Phys. **32**, L280 (1993).

[8]S. A. Majetich, J. O. Artman, M. E. McHenry, N. T. Nuhfer, and S. W. Staley, Phys. Rev. B **48**, 16 845 (1993).

[9]R. S. Ruoff, R. Malhotra, D. L. Huestis, D. S. Tse, and D. C. Lorents, Nature **362**, 141 (1993).

[10]D. S. Bethune, C. H. Kiang, M. S. de Vries, G. Gorman, R. Savoy, J. Vazquez, and R. Beyers, Nature **363**, 605 (1993).

[11]B. D. Cullity, *Introduction to Magnetic Materials* (Addison-Wesley, Reading, MA, 1972).

[12]F. E. Luborsky, J. Appl. Phys. **32**, 171S (1961).

[13]C. P. Bean and J. D. Livingston, J. Appl. Phys. **30**, 120S (1959).

[14]I. S. Jacobs and C. P. Bean, in *Magnetism,* edited by G. T. Rado and H. Suhl (Academic, New York, 1963), Vol. 3.

[15]W. D. Doyle and P. J. Flanders, in *International Conference of Magnetism, Nottingham, 1964* (The Institute of Physics and the Physical Society, Bristol, 1965), pp. 751–755.

[16]W. A. Sucksmith and J. E. Thompson, Proc. R. Soc. London Ser. A **225**, 362 (1954).

[17]R. F. Ziolo, E. P. Giannelis, B. A. Weinstein, M. P. O'Horo, B. N. Ganguly, V. Mehrotra, M. W. Russell, and D. R. Huffman, Science **257**, 219 (1992).

[18]J. K. Vassiliou, V. Mehotra, M. W. Russell, E. P. Giannelis, R. D. McMichael, R. D. Shull, and R. F. Ziolo, J. Appl. Phys. **73**, 5109 (1993).

[19]For a comparison see E. M. Brunsman, R. Sutton, E. Bortz, S. Kirkpatrick, K. Midelfort, J. Williams, P. Smith, M. E. McHenry, S. A. Majetich, J. O. Artman, M. De Graef, and S. W. Staley, MMM 1993 Conference, Minneapolis, Minn. [J. Appl. Phys. (to be published)].

[20]W. H. Meiklejohn, J. Appl. Phys. **29**, 454 (1958).

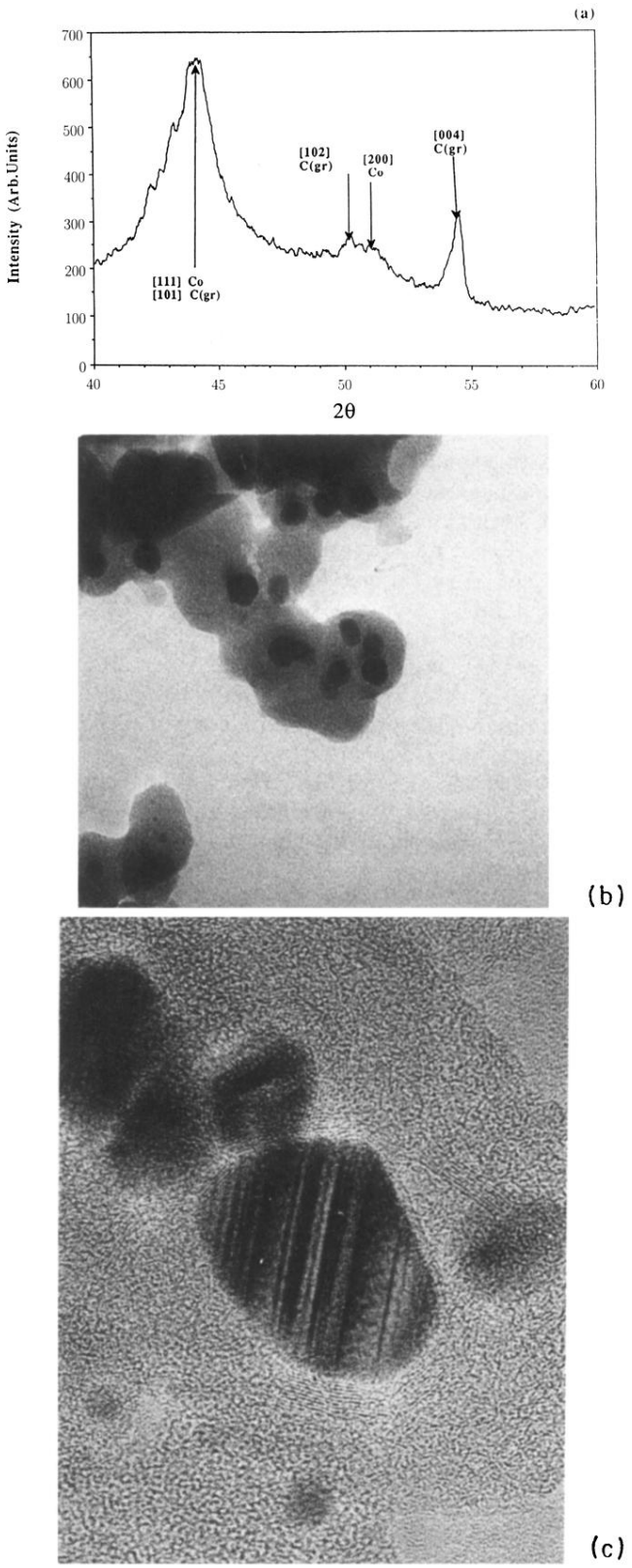

FIG. 1. (a) X-ray diffraction pattern of the magnetically separated powder taken with a Rigaku diffractometer using copper K_α and K_β radiation fcc Co and hexagonal graphite peaks are identified. (b) Transmission electron micrograph of a cobalt nanocrystallite enclosed by several graphitic sheets, taken with a JEOL 400 high-resolution TEM. (c) HRTEM micrograph of an individual Co nanocrystallite showing stacking faults.